Journal of Hydrology 677 (2026) 136012

Contents lists available at ScienceDirect

Journal of Hydrology

journal homepage: www.elsevier.com/locate/jhydrol

Research papers

The impact of seasonal hydroclimatic variability and vegetation dynamics on long-term nutrient trends – Evidence from an agriculture-dominated watershed draining to the Baltic Sea

Beata Plutova [a,*], Carlos Gonzales-Inca [a], Elham Kakaei Lafdani [a], Iiro Seppä [a], Elina Kasvi [a], Maria Kämäri [b], Petteri Alho [a], Ville Kankare [a,c]

[a] *Department of Geography and Geology, University of Turku, Vesilinnantie 5, FI-20014 Turku, Finland*
[b] *Finnish Environment Institute Syke, Latokartanonkaari 11, 00790 Helsinki, Finland*
[c] *Finnish Geospatial Research Institute FGI, Vuorimiehentie 5, FI-02150 Espoo, Finland*

ARTICLE INFO

This manuscript was handled by Huaming Guo, with the assistance of Lei Chen, Associate Editor

Keywords:
Nitrogen
Phosphorous
Hydroclimatic variability
Vegetation dynamics
Seasonal patterns

ABSTRACT

Excess nutrient loads, particularly nitrogen (N) and phosphorus (P), play a significant role in the degradation of global water quality and aquatic ecosystems. The amount of these nutrients in rivers is significantly affected by the increasing hydroclimatic variability, coupled with changes in land use intensity. This study assessed trends over 30 years in total nitrogen (TN) and total phosphorus (TP) in the Aurajoki catchment, Southwest Finland, and evaluated how land use intensity and seasonal hydroclimatic variability influence nutrient dynamics. The utilized data consisted of long-term monitoring records of nutrient concentrations, discharge, temperature, precipitation, and the Landsat imagery series. Prior to the analyses, the Standardized Precipitation Index (SPI), Accumulated Winter Season Severity Index (AWSSI), and Normalized Difference Vegetation Index (NDVI) were used to characterize hydroclimatic variability and land use intensity. Data were analyzed using Mann-Kendall statistics to assess trends and generalized additive mixed models (GAMMs) to evaluate the impact of land use intensity and hydroclimatic variability. Results showed a decrease in annual TN concentrations and TN loads, while TP trends remained stable. The seasonal trend test revealed significant TN and TP increases in fall and decreases in spring. The modelling results revealed that NDVI had a significant impact only on nutrient concentrations, whereas the effects of hydroclimatic class were limited to nutrient loads and varied according to different combinations of season and NDVI. These findings highlight the relevance of seasonal hydroclimatic variability and land use intensity when assessing nutrient dynamics, particularly in the context of climate change and water protection strategies.

1. Introduction

Nutrient enrichment of rivers, lakes, and coastal waters remains a major global environmental problem. Excessive inputs of nitrogen (N) and phosphorus (P) drive eutrophication, harmful algal blooms, and biodiversity loss, resulting in widespread degradation of aquatic ecosystems (Dodds and Smith, 2016; Ngatia et al., 2019; Wurtsbaugh et al., 2019). Therefore, identification and targeting the most critical nutrient source areas and understanding factors regulating the magnitude of nutrient pollution reaching the rivers is crucial for effective water-quality management and the protection of aquatic ecosystem health (Liu et al., 2025; McDowell et al., 2025; Sun et al., 2024).

Land use intensity is one of the key drivers of nutrient loading, as it influences both nutrient sources and hydrological pathways within catchments (Kronvang et al., 2020; Schürings et al., 2024). In boreal and hemiboreal regions, agricultural practices play a particularly important role. Short growing seasons and long non-growing periods limit annual crop uptake and increase the vulnerability of soils to nutrient losses. Additionally, fertilizer management and tillage practices strongly influence nutrient export (Liu et al., 2019a). For example, optimizing fertilizer application and reducing soil tillage have been shown to significantly decrease N and P loading in intensively farmed areas of Finland (Huttunen et al., 2021; Uusitalo et al., 2024). In contrast, forestry generally contributes less to catchment scale nutrient loads.

* Corresponding author.
E-mail address: beplut@utu.fi (B. Plutova).

https://doi.org/10.1016/j.jhydrol.2026.136012
Received 6 February 2026; Received in revised form 6 June 2026; Accepted 10 July 2026
Available online 11 July 2026

Although intensive management and drainage can increase nutrient export locally, especially in peatland and headwater systems (Marttila et al., 2018; Nieminen et al., 2018; Rankinen et al., 2023). Furthermore, urban areas are another non-point source of pollutants as they lead to increased surface runoff which creates additional transport of sediment and nutrients from landscape into rivers (Giri and Qiu, 2016).

At the same time, hydroclimatic variability, including fluctuations in precipitation, temperature, snowmelt patterns, and discharge, plays a critical role in controlling nutrient mobilization and transport within river catchments (Bamal et al., 2025). In boreal and hemiboreal catchments, a large share of annual nutrient loading occurs due to snowmelt runoff (Liu et al., 2019a). Snowmelt runoff strongly influence nutrient transport to surface and ground waters, causing erosion and soil fertility degradation (Hoffman et al., 2019). Moreover, increased rainfall, especially outside the growing season when vegetation cover is reduced, can also generate high nutrient loads (Øygarden et al., 2014). Climate change is expected to amplify these dynamics, particularly in Northern Europe, where warmer and wetter conditions are expected (IPCC, 2013, 2007). Specifically, in southern and central Finland, this will significantly alter the seasonality of runoff and floods, with increasing floods during fall and winter and diminishing floods in spring (Veijalainen et al., 2010). Furthermore, the annual average temperature in Finland is expected to increase by 1–4°C by the end of the 21st century. In winter, the increase will be 3–9°C, and in summer, 1–5°C. Annual precipitation is predicted to increase by 12% in winter and 5% in summer (Ruosteenoja and Jylhä, 2021).

Current practices for investigating nutrient transport in boreal and hemiboreal regions rely on combining long-term water quality monitoring with catchment-scale hydrological and nutrient modelling to quantify nutrient loads, identify transport pathways, and assess spatial and temporal variability. In Finland, long-term monitoring datasets and modelling based assessments have been widely used to detect trends in nutrient transport in relation to climate change and diffuse agricultural inputs, effectiveness of water protection measures, and societal and political drivers (Gonzales-Inca et al., 2016; Huttunen et al., 2021; Knuuttila et al., 2017; Räike et al., 2019; Rankinen et al., 2019, 2016; Uusheimo et al., 2020). Using the long-term datasets, several studies have also shown that catchment characteristics such as landscape patterns, soil type, topography, and buffer zones, play an important role in regulating nutrient losses and transport processes (Gonzales-Inca et al., 2015; Röman et al., 2018; Varanka et al., 2015; Varanka and Hjort, 2017). However, these approaches often provide limited insight into seasonal controls and rapidly varying processes, particularly vegetation dynamics and short term hydroclimatic variability.

To address this limitation, this study integrates long-term nutrient observations with remotely sensed vegetation indicator (NDVI) and hydroclimatic indices and classification. A Generalized Additive Mixed Model (GAMM) framework is then applied to quantify nonlinear and seasonal relationships between environmental drivers and nutrient dynamics. The analysis examines both annual and seasonal dynamics of total nitrogen (TN) and total phosphorus (TP). The study focuses on the Aurajoki catchment in southwestern Finland, an agriculturally dominated basin that contributes substantially to nutrient loading in the Archipelago Sea, one of the last major eutrophication hotspots in Finnish coastal waters (Laamanen, 2025).

The study specific objectives are to (i) quantify long-term annual and seasonal trends (1990–2024) in TN and TP concentrations, loads, and hydroclimatic variables, and (ii) assess how hydroclimatic variability and land use intensity influence nutrient dynamics using a GAMM framework. By statistically linking vegetation dynamics and hydroclimatic indices, this study provides a comprehensive data-driven perspective on nutrient runoff and management in hemiboreal catchment under changing weather conditions.

2. Materials and methods

2.1. Study area

The Aurajoki catchment is situated in Southwest Finland and covers an area of 875 km^2. This study focuses on the Aura 54 sub-catchment, which drains 731 km^2 of the total catchment area (Fig. 1). The Aura 54 sub-catchment was selected because the river monitoring station located there provides long-term, seasonally stratified measurements for TN and TP, ensuring robust temporal coverage for nutrient load trend analysis. The drainage is into the Archipelago Sea, which is one of the sub-basins of the Baltic Sea (Fig. 1). The Archipelago Sea has a moderate ecological class (Laamanen, 2025), and the ecological class of the Aurajoki River is poor.

Situated in the hemiboreal climate zone, Köppen Dfb (Jylhä et al., 2010), the region experiences marked seasonal hydroclimatic variability. For the climate reference period 1991–2020, the catchment received an annual average precipitation of 646 mm, including 110 mm as snow, and experienced an average air temperature of 5.64°C. During the same period, annual average runoff measured at the Halinen dam was 289 mm (Seppä et al., n.d.). The river typically freezes each winter, with exceptions only in 2007–2008 and 2019–2020 (Norrgård and Helama, 2022), highlighting the sensitivity of hydrological processes to climatic anomalies.

The Aurajoki catchment is primarily covered by forestry and agriculture. Forestry covers approximately 53% and agricultural land 37% of the area (Table A1). Crops such as AIV fodder, cereals, and sugar beet dominate the fields, while pork and chicken production are key livestock activities (LUKE, 2025a, 2025b). The main soil texture in the catchment is clay (47%), followed by bedrock (33%), peatland (10%), till (6%), and coarse soils (3%) (Seppä et al., n.d.). The overall baseflow index (BFI) for the studied catchment is 0.27, as estimated using the Lyne and Hollick filter method (Li et al., 2013; Nagy et al., 2024). This relatively low BFI indicates that the catchment is hydrologically flashy and has limited groundwater storage capacity. Consequently, streamflow is likely dominated by surface runoff generated from snowmelt and rainfall events.

2.2. Data

2.2.1. Water quality data

In this study, long-term water quality data from the Aurajoki catchment were used. Water quality data were obtained from the open environmental information systems maintained by the Finnish Environment Institute (Syke) (Syke, 2025a) for the river monitoring station Aura 54 (Fig. 1). The water quality variables included TN and TP concentrations. A total of 1282 TN samples and 1278 TP samples were collected during the period from 1990 to 2024, with sampling primarily conducted during spring and autumn.

2.2.2. Hydrometeorological data

Daily hydrometeorological data between 1990 and 2023 were obtained from the CAMELS-FI dataset (Seppä et al., n.d.). The data consisted of discharge, catchment-averaged precipitation, and mean temperature for the monitoring station at Halinen dam (Fig. 1). Catchment geometry was obtained from a 10 m x 10 m digital elevation model (DEM) of the National Land Survey of Finland (NLS) (NLS, 2016), using the methodology described in Seppä et al., (n.d). Since the discharge and water quality measurements were taken at two separate but proximate locations, we adjusted the discharge values by multiplying them by the areal ratio of the Aura 54 and Halinen sub-catchments (0.971) to ensure comparability.

2.2.3. Land use data

Dominant land cover types within the Aura 54 sub-catchment were derived as areal portions from all available Finnish editions of the

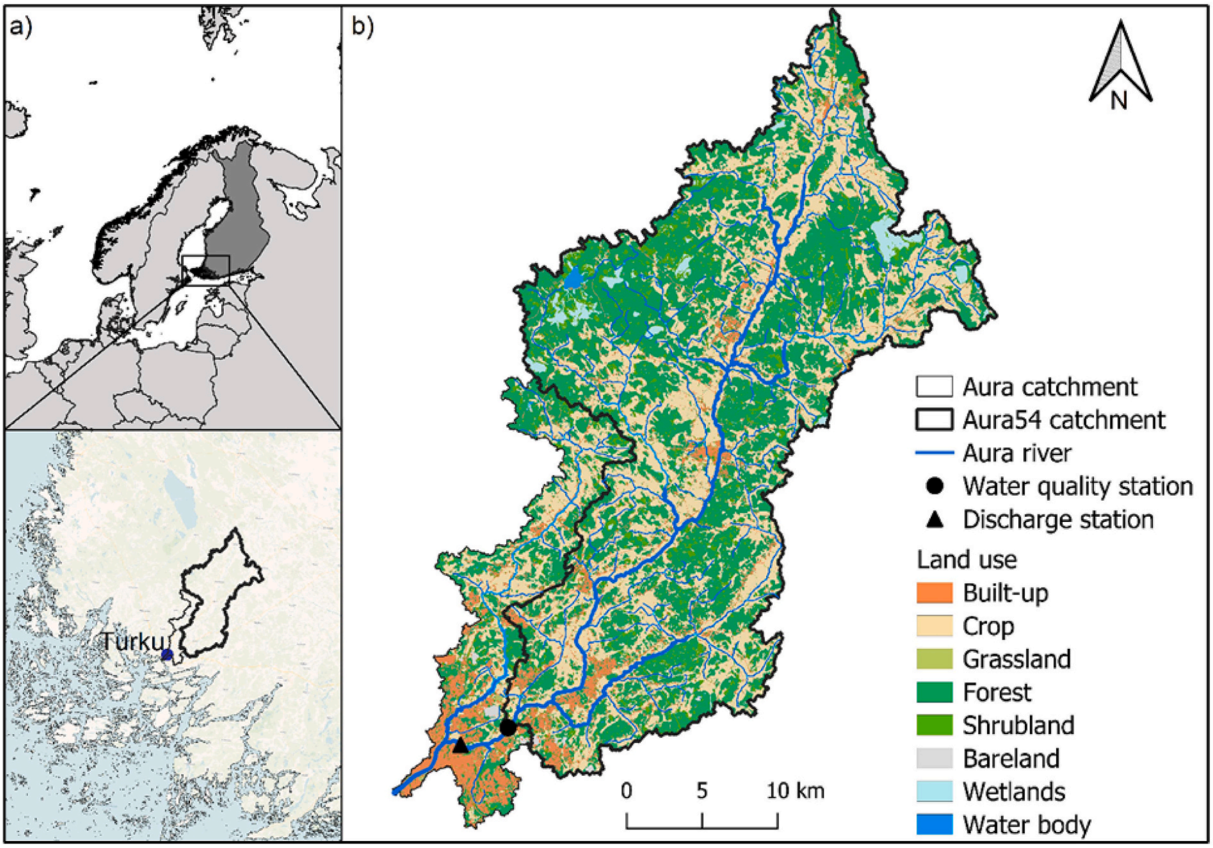

Fig. 1. Study area overview. (a) Location of the Aurajoki catchment within northern Europe and Finland. (b) Aurajoki catchment with the locations of monitoring stations, major land use types, and the delineated study sub-catchment area for Aura 54.

CORINE Land Cover (CLC) dataset, corresponding to the years 2000, 2006, 2012, and 2018 (Table A1; (Syke, 2025b)). The Finnish CLC products offer higher spatial resolution and a smaller minimum mapping unit compared to the pan-European CLC datasets, thereby providing more detailed land cover information suitable for catchment-scale analysis. Vegetation cover dynamics were analyzed using the Normalized Difference Vegetation Index (NDVI), calculated from imagery collected from the Landsat satellite series (Landsat 5, 7, 8 and 9).

2.3. Methods

A conceptual overview of the study framework is shown in Fig. 2,

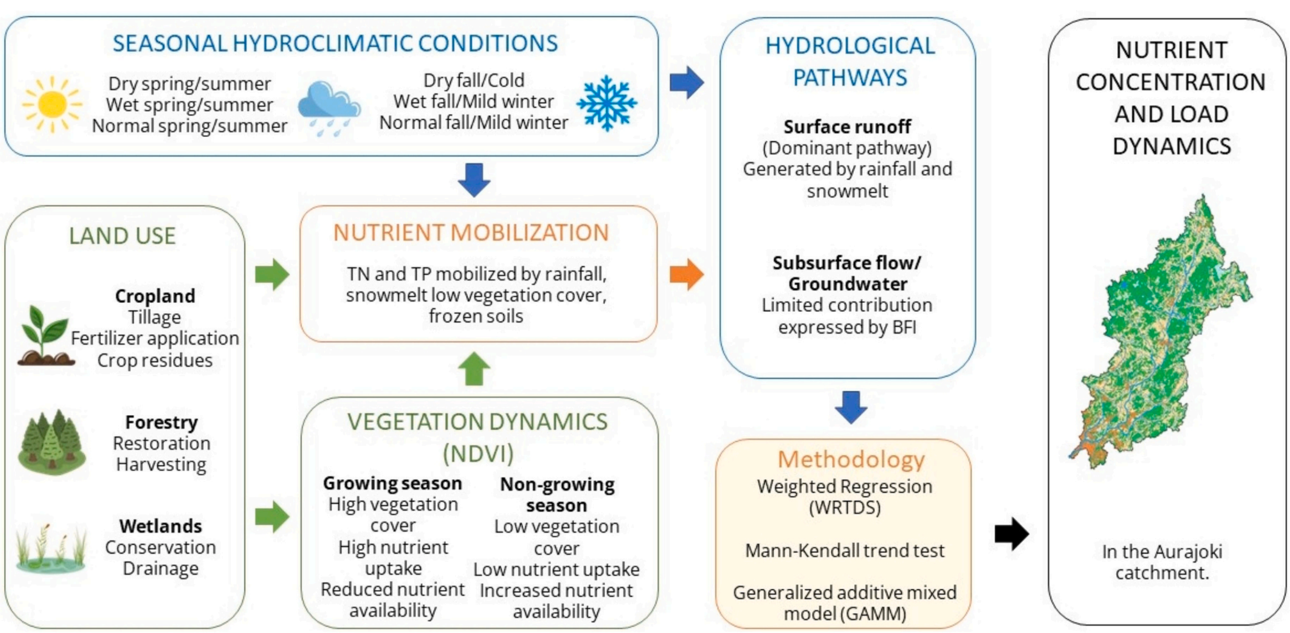

Fig. 2. Conceptual framework of nutrient mobilization and the effect of hydroclimatic conditions in the Aurajoki catchment.

illustrating the interactions between key drivers and processes influencing nutrient dynamics in the Aurajoki catchment, as well as the applied methodological approach.

2.3.1. Nutrient concentrations and loads

Nutrient loads were calculated using the Weighted Regressions on Time, Discharge, and Season (WRTDS) method, developed by (Hirsch et al., 2010). This approach uses observed concentration data to model how nutrient concentrations vary with streamflow, time, and season. All calculations were performed using the EGRET package (Hirsch and De Cicco, 2015) in R (R Core Team, 2025). The model estimates daily concentrations over the full period of record by fitting a regression equation that accounts for long-term trends (time in years), seasonal patterns (time of year), and flow conditions (discharge) as:

$$\ln(c) = \beta_0 + \beta_1 t + \beta_2 \ln(Q) + \beta_3 \sin(2\pi t) + \beta_4 \cos(2\pi t) + \varepsilon \quad (1)$$

Where the β values are fitted coefficients, c is the concentration (mg/l), Q (m^3/s) is discharge, t is the time in years, and ε is the unexplained variation. The weighting process assigns a weight to each observation in the dataset based on its proximity to the selected values of time (t_0) and discharge (Q_0). Observations that are farther from these values receive lower weights. A weighted regression is then performed using these weights, and the resulting coefficients are used to estimate the expected value of ln(c) for that specific time and discharge.

Subsequently, the daily load is calculated by multiplying the estimated daily concentration by the respective daily mean discharge. The method provides not only estimates of concentrations and loads but also flow–normalized estimates of concentrations and loads for the entire period of record. Flow-normalization removes the influence of the temporal variability in discharge by considering the discharge on any given day as a random sample from the range of discharges that could occur on that day. Annual and monthly nutrient loads were calculated by summing up daily values, while annual and monthly means for concentration were derived from their respective daily values.

2.3.2. The NDVI estimation

NDVI values were estimated using the standard formula:

$$NDVI = (NIR - Red) / (NIR + Red) \quad (2)$$

Where *NIR* is near-infrared reflectance and *Red* is visible red reflectance, yielding values between -1 and 1 (Huang et al., 2021). Higher NDVI values (closer to 1) indicate dense, healthy vegetation with high photosynthetic activity, whereas lower values (near 0 or negative) correspond to sparse vegetation, bare soil, or water surfaces. To ensure consistency across different Landsat sensors, we used atmospherically corrected surface reflectance imagery. Cloud and water pixels were masked to generate cloud-free image composites for three seasonal periods: spring (April–May), summer (June–July), and fall (August–September), for each year between 1990 and 2024. NDVI values were not calculated for winter due to limited vegetation activity and frequent cloud cover.

Subsequently, for each season, the mean NDVI was calculated for dominant land cover classes (cropland, forest, and wetland) within the Aura 54 catchment. All image processing and analysis were conducted using the Google Earth Engine cloud platform (Gorelick et al., 2017). These seasonal NDVI values were used as predictors in GAMMs to assess the influence of vegetation dynamics on TN and TP.

2.3.3. Hydroclimatic year classification

To define hydroclimatic year classes, two indices were combined: the Standardized Precipitation Index (SPI) and the Accumulated Winter Season Severity Index (AWSSI). The SPI quantifies precipitation anomalies over specific timescales, enabling assessment of wet and dry conditions (Mckee et al., 1993). SPI was applied to characterize seasonal conditions for spring (March–May), summer (June–August), and fall (September–November). Winter conditions (December–February) were characterized using AWSSI, which integrates temperature extremes, snowfall, snow depth, and the duration of winter weather to generate a comprehensive, site-specific index of winter severity (Boustead et al., 2015).

By combining these two indices, both thermal and moisture-related drivers of hydroclimatic variability were captured across all seasons. Each year from 1990 to 2023 was then assigned to a hydroclimatic class based on dominant seasonal patterns, using either spring/summer or fall/winter conditions as the basis, along with a “normal year” category. This classification reflects typical hydroclimatic conditions in Finland, such as average spring, summer, and fall seasons combined with a cold or very cold winter. The normal year category served as the reference hydroclimatic class in the GAMMs, providing a baseline for evaluating the influence of seasonal climate variability on TN and TP.

As a result, two main hydroclimatic classification schemes were created, each consisting of four subclasses: one based on spring/summer conditions and one on fall/winter conditions. In some cases, fall/winter categories were adapted to ensure consistency in the four-class structure. The final classification for the period 1990–2023 is presented in Table 1.

2.3.4. Trends in the nutrient and hydroclimatic time series

The Mann–Kendall and seasonal Kendall tests (Hirsch, 1982, 1991) were used to assess monotonic trends in nutrients and hydroclimatic time series. These tests were applied to both non-normalized and flow-normalized estimated loads and concentrations. The analysis was conducted using the Kendall (McLeod, 2011) and trend (Pohlert, 2020) packages in R (R Core Team, 2025). The test statistic was computed using the following formula:

$$S = \sum_{k=1}^{n-1} \sum_{j=k+1}^{n} sgn\left(x_{ij} - x_{jk}\right) \quad (3)$$

Where x_j and x_k are the annual values in years j and $k, j > k$, respectively. The magnitude of detected trends was quantified using the Theil–Sen slope estimator (Hirsch, 1982).

2.3.5. Generalized additive mixed model (GAMM)

GAMM was used to evaluate the influence of seasonal hydroclimatic variability and NDVI on nutrient concentrations and loads. The GAMM enables the identification and quantification of nonlinear and season-dependent relationships between environmental drivers and nutrient responses, which cannot be captured using simple linear models. The model was implemented using the *mgcv* package (Wood, 2000) in R (R Core Team, 2025). Separate models were constructed for each seasonal configuration, combining hydroclimatic class and season-specific NDVI values. The following combinations were: i) spring/summer hydroclimatic class with spring NDVI, ii) spring/summer hydroclimatic class with summer NDVI, iii) fall/winter hydroclimatic class with summer NDVI, and iv) fall/winter hydroclimatic class with fall NDVI. Each model was applied to both nutrient concentrations and loads, allowing interpretation of seasonal land use effects and nutrient transport dynamics. Prior to model fitting, principal component analysis (PCA) was applied to NDVI values (Jolliffe, 2011) to reduce multicollinearity among land-cover NDVI variables (forest, cropland, wetland) and improve numerical stability. The first two principal components (PC1 and PC2) were retained, explaining the majority of variance (>90%) and representing (i) overall catchment greenness (PC1) and (ii) the contrast between forest/wetland and cropland greenness (PC2). These components were used as smooth predictors in the GAMMs. The general form of the model was:

$$y = s(NDVI_{PC1}, k = 5) + s\left(NDVI_{PC2}, k = 5\right) + H + s(Season, bs = "re") \quad (4)$$

Where y is either TN or TP concentration/load, s () are smooth terms for NDVI principal components (PC1, PC2) fitted using thin plate regression splines with a maximum basis dimension of k = 5, H is

Table 1
The resulting hydroclimatic year classification for the period 1990–2023.

Year	Spring (SPI)	Summer (SPI)	Fall (SPI)	Winter (AWSSI)	Hydroclimatic class (Spring/Summer)	Hydroclimatic class (Fall/Winter)
1990	Normal	Normal	Normal	Cold	Normal year	Normal year
1991	Normal	Normal	Normal	Cold	Normal year	Normal year
1992	Normal	Normal	Wet	Mild	Normal Spring/Summer	Wet Fall/Mild Winter
1993	Dry	Dry	Normal	Mild	Dry Spring/Summer	Normal Fall/Mild Winter
1994	Wet	Wet	Dry	Very cold	Wet Spring/Summer	Dry Fall/Cold Winter
1995	Wet	Wet	Normal	Mild	Wet Spring/Summer	Normal Fall/Mild Winter
1996	Normal	Normal	Normal	Very cold	Normal year	Normal year
1997	Normal	Normal	Normal	Very cold	Normal year	Normal year
1998	Normal	Normal	Normal	Cold	Normal year	Normal year
1999	Normal	Normal	Normal	Cold	Normal year	Normal year
2000	Normal	Normal	Normal	Cold	Normal year	Normal year
2001	Normal	Normal	Normal	Mild	Normal Spring/Summer	Normal Fall/Mild Winter
2002	Dry	Dry	Wet	Cold	Dry Spring/Summer	Wet Fall/Mild Winter*
2003	Normal	Normal	Dry	Very cold	Normal Spring/Summer	Dry Fall/Cold Winter
2004	Normal	Normal	Dry	Very cold	Normal Spring/Summer	Dry Fall/Cold Winter
2005	Dry	Dry	Normal	Mild	Dry Spring/Summer	Normal Fall/Mild Winter
2006	Normal	Normal	Normal	Cold	Normal year	Normal year
2007	Normal	Normal	Wet	Mild	Normal Spring/Summer	Wet Fall/Mild Winter
2008	Normal	Normal	Normal	Mild	Normal Spring/Summer	Normal Fall/Mild Winter
2009	Dry	Dry	Wet	Mild	Dry Spring/Summer	Wet Fall/Mild Winter
2010	Wet	Wet	Normal	Very cold	Wet Spring/Summer	Normal Fall/Mild Winter*
2011	Normal	Normal	Normal	Very cold	Normal year	Normal year
2012	Normal	Normal	Normal	Cold	Normal year	Normal year
2013	Normal	Normal	Normal	Very cold	Normal year	Normal year
2014	Normal	Normal	Normal	Mild	Normal Spring/Summer	Normal Fall/Mild Winter
2015	Wet	Wet	Dry	Cold	Wet Spring/Summer	Dry Fall/Cold Winter
2016	Normal	Normal	Normal	Mild	Normal Spring/Summer	Normal Fall/Mild Winter
2017	Nor mal	Normal	Dry	Mild	Normal Spring/Summer	Dry Fall/Cold Winter *
2018	Dry	Dry	Normal	Cold	Dry Spring/Summer	Normal Fall/Mild Winter*
2019	Normal	Normal	Normal	Very cold	Normal year	Normal year
2020	Wet	Wet	Wet	Mild	Wet Spring/Summer	Wet Fall/Mild Winter
2021	Wet	Wet	Normal	Cold	Wet Spring/Summer	Normal Fall/Mild Winter*
2022	Normal	Normal	Normal	Cold	Normal year	Normal year
2023	Normal	Normal	Normal	Cold	Normal year	Normal year

Note: * Customized fall/winter hydroclimatic year classes.

hydroclimatic class (spring/summer or fall/winter; Table 1), and bs="re" indicates a random effect for season. Models were estimated using Restricted Maximum Likelihood (REML) with automatic term selection enabled.

3. Results

3.1. Trends in nutrient concentrations and loads

In general, there was a decreasing trend in annual TN concentrations and loads, while annual TP showed no significant trends over the period from 1990 to 2024 (Tables 2 and 3). Both flow-normalized and raw TN concentrations showed statistically significant decreasing trends (Table 2), whereas the same decreasing trend was found only in flow-normalized TN loads (Table 3). These trends in annual TN and TP concentrations and loads are further illustrated in Fig. 3.

Seasonal trend analyses revealed more pronounced patterns in nutrient concentrations and loads (Tables 2 and 3). During winter, a significant decline was observed in flow-normalized TN concentration, while there was an increase in flow-normalized TP load. In spring, both non– and flow-normalized TN and TP concentrations and loads exhibited significant decreasing trends. Whereas in fall, the nutrient concentrations and loads showed increasing trends. In summer, there was a significant increase, but only for flow-normalized TN and TP loads (Table 3).

3.2. Trends in hydroclimatic variables

Trend analysis of hydroclimatic variables during 1990–2023 revealed a significant annual trend only for temperature. In contrast, seasonal analysis showed significant trends in all variables (Table 4). Discharge exhibited a significant decrease in spring and an increase in fall, indicating a shift in flow regimes. However, precipitation showed only a marginally significant increase in summer. In addition to this, the

Table 2
Mann – Kendall results for estimated TN and TP concentrations: annual and seasonal values between 1990 and 2024 (flow-normalized and non-normalized).

	Non – normalized concentration						Flow – normalized concentration					
	TN			TP			TN			TP		
Season	Slope (µg/l/y)	*p*	Trend	Slope(µg/l/y)	*p*	Trend	Slope(µg/l/y)	*p*	Trend	Slope(µg/l/y)	*p*	Trend
Annual	−13.2	**	↘	0.23	–	–	−17.5	***	↘	0.02	–	–
Winter	−1.33	–	–	0.09	–	–	−1.74	*	↘	0.02	–	–
Spring	−3.50	***	↘	−0.44	**	↘	−3.22	***	↘	−0.42	**	↘
Summer	−1.58	–	–	−0.07	–	–	−2.11	–	–	0.03	–	–
Fall	3.43	**	↗	0.77	***	↗	2.93	**	↗	0.79	***	↗

Significance codes: *p $<$ 0.05, **p $<$ 0.01, ***p $<$ 0.001.
Trend: ↘ Decrease– No change ↗ Increase.

Table 3
Mann–Kendall trend results for estimated TN and TP loads: annual and seasonal values between 1990 and 2024 (flow-normalized and non-normalized).

	Non – normalized load						Flow – normalized load					
	TN			TP			TN			TP		
Season	Slope(t/y)	*p*	Trend	Slope(t/y)	*p*	Trend	Slope(t/y)	*p*	Trend	Slope(t/y)	*p*	Trend
Annual	−2.57	–	–	0.18	–	–	−0.54	*	↘	0.049	–	–
Winter	0.19	–	–	0.01	–	–	0.02	–	–	0.003	**	↗
Spring	−0.76	***	↘	−0.06	***	↘	−0.08	***	↘	−0.006	*	↘
Summer	−0.01	–	–	−3e-04	–	–	0.01	**	↗	0.001	***	↗
Fall	0.60	***	↗	0.05	***	↗	0.12	***	↗	0.013	***	↗

Significance codes: *$p < 0.05$, **$p < 0.01$, ***$p < 0.001$.
Trend: ↘ Decrease – No change ↗ Increase.

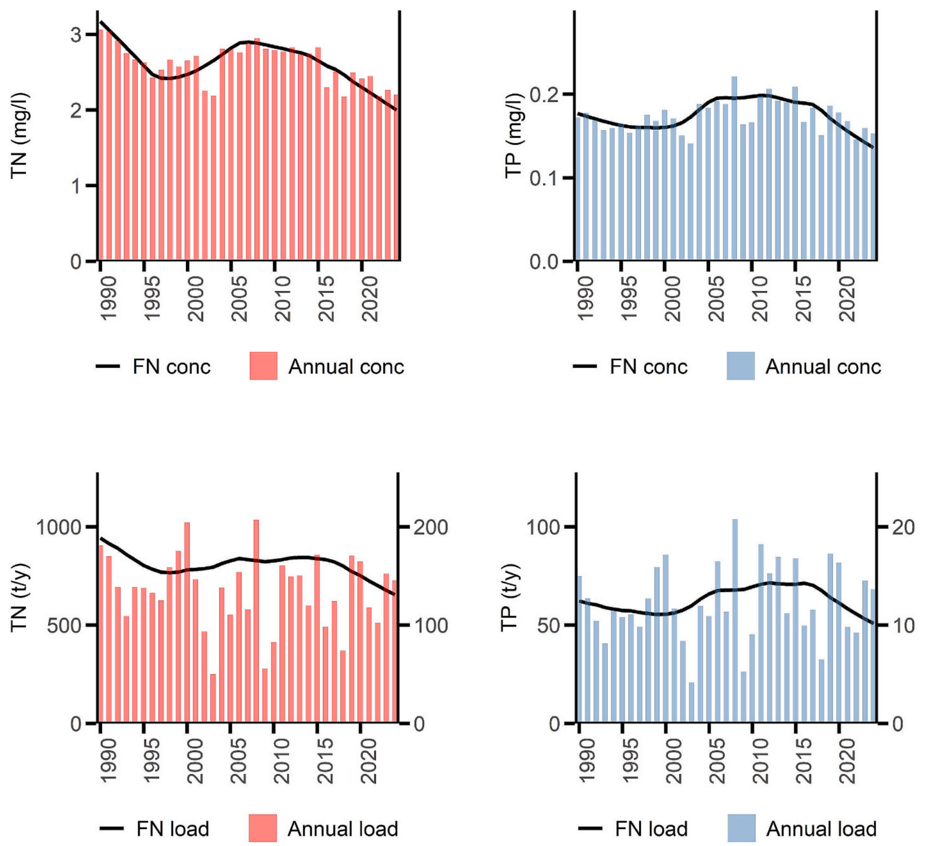

Fig. 3. Long-term trends (1994 – 2024) for flow-normalized (FN) and non – normalized (Annual) TN and TP concentrations, and loads.

Table 4
Mann–Kendall trend results for discharge, temperature, and precipitation: annual and seasonal values (1990 – 2023).

	Discharge (m^3/s)			Temperature (°C)			Precipitation (mm)		
Season	Slope (m^3/s/y)	*p*	Trend	Slope(°C/y)	*p*	Trend	Slope (mm/y)	*p*	Trend
Annual	7.50	–	–	0.03	*	↗	−0.001	–	–
Winter	1.02	–	–	0.03	**	↗	0.002	–	–
Spring	−2.39	**	↘	0.15	***	↗	−0.001	–	–
Summer	−0.02	–	–	0.02	***	↗	0.007	+	↗
Fall	2.37	***	↗	−0.12	***	↘	0.003	–	–

Significance codes: +$p < 0.1$, *$p < 0.05$, **$p < 0.01$, ***$p < 0.001$.
Trend: ↘ Decrease – No change ↗ Increase.

temperature increased significantly in winter, spring, and summer but declined in fall. This temperature trend in fall may be attributed to the definition of the fall season (September–November), during which monthly mean temperatures were 11°C (September), 5°C (October), and 1°C (November), respectively.

However, when analyzed individually, September showed a significantly increasing temperature trend, October showed no trend, and November exhibited a marginally significant increase (Table A2). These results suggest that the observed seasonal decline is a result of aggregating months with different temperatures, rather than an actual consistent decrease across the fall season.

3.3. The impact of land use intensity and hydroclimatic variability on nutrients – GAMMs

3.3.1. Model performance and random effect

Overall, the GAMMs explained a moderate proportion of variability in nutrient concentrations and loads. For TN concentration models, adjusted R^2 values ranged from 0.32 to 0.35, with 35–39% of the deviance explained. TP concentration models had adjusted R^2 values between 0.42 and 0.45, explaining 44–48% of the deviance. Similarly, TN load models showed adjusted R^2 values of 0.44–0.46 and 46–48% deviance explained, while TP load models ranged from 0.40 to 0.42, explaining 42–44% of the deviance. Across all models, the highest adjusted R^2 and deviance explained were associated with combinations of spring/summer hydroclimatic classes and NDVI from spring or summer. Model diagnostics indicated residual autocorrelation in the GAMMs for TN concentration, whereas TP concentration and all load models did not exhibit this issue. These results indicate that seasonal hydroclimatic variability and land use intensity, particularly during spring and summer, are important drivers of nutrient dynamics.

The random effect for season was highly significant in all GAMMs ($p < 0.001$; Tables 5 and 6). This indicates systematic differences in nutrient concentrations and loads between seasonal groups after accounting for NDVI and hydroclimatic class. Seasonal effects are expressed on the scale of the response variable and represent deviations from the model intercept. Spring and summer showed positive deviations, whereas fall exhibited the strongest negative deviations, particularly for TN. Winter effects were close to zero, indicating minimal deviation from baseline conditions (Fig. 4).

3.3.2. NDVI and hydroclimate effects on nutrient concentrations and loads

Overall, the GAMM results revealed a clear separation between the controls on nutrient concentrations and loads. Vegetation activity, represented by NDVI, was significant only in the concentration models, whereas hydroclimatic variability dominated nutrient load responses (Tables 5 and 6). This indicates that land use–related vegetation dynamics primarily regulate nutrient availability, while hydrological processes primarily control nutrient transport.

Based on PCA loadings, the NDVI components ($NDVI_{PC1}$, $NDVI_{PC2}$) were interpreted as indicators of catchment greenness. $NDVI_{PC1}$ represented overall vegetation greenness or vigor, while $NDVI_{PC2}$ captured the contrast between forest/wetland and cropland. NDVI effects therefore reflect the influence of vegetation activity and land use composition on nutrient concentrations after accounting for hydroclimatic conditions and seasonal variability.

The concentration models further revealed stronger vegetation effects on TN than TP (Table 5). NDVI effects on TN were significant across all seasonal models but varied in strength and form. In the spring/summer – spring NDVI model, TN showed a significant nonlinear response to $NDVI_{PC1}$, suggesting a transition from nutrient mobilization to plant uptake during the growing season. In the spring/summer – summer NDVI model, $NDVI_{PC1}$ remained significant with an approximately linear association, while land-use contrasts, $NDVI_{PC2}$, showed a stronger linear effect. A similarly strong $NDVI_{PC2}$ effect was observed in the fall/winter–summer NDVI model, highlighting the importance of vegetation composition during summer. In the fall/winter – fall NDVI model, TN showed a significant linear association with $NDVI_{PC1}$, dominated by forest and wetland (loadings ≈ 0.66) with a smaller contribution from cropland (≈ 0.35). In contrast, NDVI effects on TP were significant only in the spring/summer – spring NDVI model, where a modest, near-linear relationship with $NDVI_{PC1}$ was observed (Table 5).

Hydroclimatic class had limited influence on concentrations, except for a negative effect of the dry spring/summer class on both TN and TP (Table 5). In contrast, hydroclimatic effects were significant in all nutrient load models (Table 6). In spring and summer, nutrient loads were significantly reduced under dry conditions, with the marginal effect of normal conditions. In fall and winter, nutrient loads were significantly reduced under normal/wet fall and mild winter conditions. Overall, the hydroclimatic effects were stronger for TN than TP loads. These results indicate that nutrient export is primarily controlled by hydrological conditions, which regulate runoff generation, connectivity, and transport processes. Additionally, intercepts in all models were significantly positive, representing the baseline mean concentration for the reference hydroclimatic class after accounting for seasonal random effects.

4. Discussion

4.1. Long-term trends in nutrient concentrations, loads and hydroclimatic variables

Eutrophication has long been a major environmental concern in the Baltic Sea and its contributing river catchments, with diffuse nutrient loading from agriculture playing a central role (HELCOM, 2023). As a result, extensive mitigation efforts have been implemented over recent decades across the region to reduce nutrient inputs from agricultural and point sources (HELCOM, 2021; WFD, 2000). These efforts have led to decreases in long-term trends, although responses have varied between nutrients and catchments (Stålnacke et al., 2014; Tattari et al., 2017). For example, TN concentrations declined notably in Denmark and Sweden following mitigation measures during 1990–2010, whereas TP trends have been more variable and strongly dependent on catchment P balance and soil type (Kyllmar et al., 2023). At the regional scale, annual flow-normalized TN and TP loads to the Archipelago Sea have declined significantly over the past 30 years (Laamanen, 2025), primarily due to improvements in wastewater treatment and fish-farming practices. Consistent with this, the observed decrease in TN concentrations and

Table 5

Summary of the GAMM predicting TN and TP concentrations, with adjusted R^2, Restricted Maximum Likelihood (REML), parameter estimates for intercept and hydroclimatic class (DSS = Dry Spring/Summer), estimated degrees of freedom (EDF) for smooth terms of NDVI principal components ($NDVI_{PC1}$, $NDVI_{PC2}$), and Season.

Model	Model response		Parameter estimates		Estimated degrees of freedom (EDF)		
TN – concentration	R^2	REML	Intercept	DSS	$NDVI_{PC1}$	$NDVI_{PC2}$	Season
spring/summer-$NDVI_{spring}$	0.32	46.11	2.66***	−0.15+	2.66***	–	2.83***
spring/summer-$NDVI_{summer}$	0.35	40.06	2.64***	−0.17*	0.85*	1.05***	2.84***
fall/winter-$NDVI_{summer}$	0.32	42.60	2.64***	–	–	1.01***	2.83***
fall/winter-$NDVI_{fall}$	0.32	42.11	2.66***	–	1.04***	–	2.83***
TP – concentration							
spring/summer-$NDVI_{spring}$	0.45	−268.37	0.18***	−0.02*	0.78*	–	2.92***
spring/summer-$NDVI_{summer}$	0.44	−267.73	0.18***	−0.01+	–	–	2.92***
fall/winter-$NDVI_{summer}$	0.42	−265.48	0.18***	–	–	–	2.91***
fall/winter-$NDVI_{fall}$	0.42	−265.15	0.18***	–	–	–	2.91***

Significance codes: +p < 0.1, *p < 0.05, **p < 0.01, ***p < 0.001.

Table 6
Summary of the GAMM predicting TN and TP loads, with adjusted R^2, Restricted Maximum Likelihood (REML), parameter estimates for intercept and hydroclimatic classes (DSS = Dry Spring/Summer, NSS = Normal Spring/Summer, WFMW = Wet Fall/Mild Winter, NFMW = Normal Fall/Mild Winter), and estimated degrees of freedom (EDF) for Season.

Model	Model response		Parameter estimates					EDF
TN − load	R^2	REML	Intercept	DSS	NSS	NFMW	WFMW	Season
spring/summer-NDVI$_{spring}$	0.46	796.09	195.06***	−84.53***	−37.13+	–	–	2.92***
spring/summer-NDVI$_{summer}$	0.46	796.09	195.06***	−84.53***	−37.13+	–	–	2.92***
fall/winter-NDVI$_{summer}$	0.44	798.41	195.06***	–	–	−44.82*	−53.16*	2.91***
fall/winter-NDVI$_{fall}$	0.44	798.41	195.06***	–	–	−44.82*	−53.16*	2.91***
TP − load								
spring/summer-NDVI$_{spring}$	0.42	502.82	18.14***	−8.41**	−3.89+	–	–	2.90***
spring/summer-NDVI$_{summer}$	0.41	502.86	18.03***	−8.27**	−3.75+	–	–	2.90***
fall/winter-NDVI$_{summer}$	0.40	504.71	18.03***	–	–	−4.46*	−5.11+	2.90***
fall/winter-NDVI$_{fall}$	0.40	504.71	18.03***	–	–	−4.46*	−5.11+	2.90***

Significance codes: +$p < 0.1$, *$p < 0.05$, **$p < 0.01$, ***$p < 0.001$.

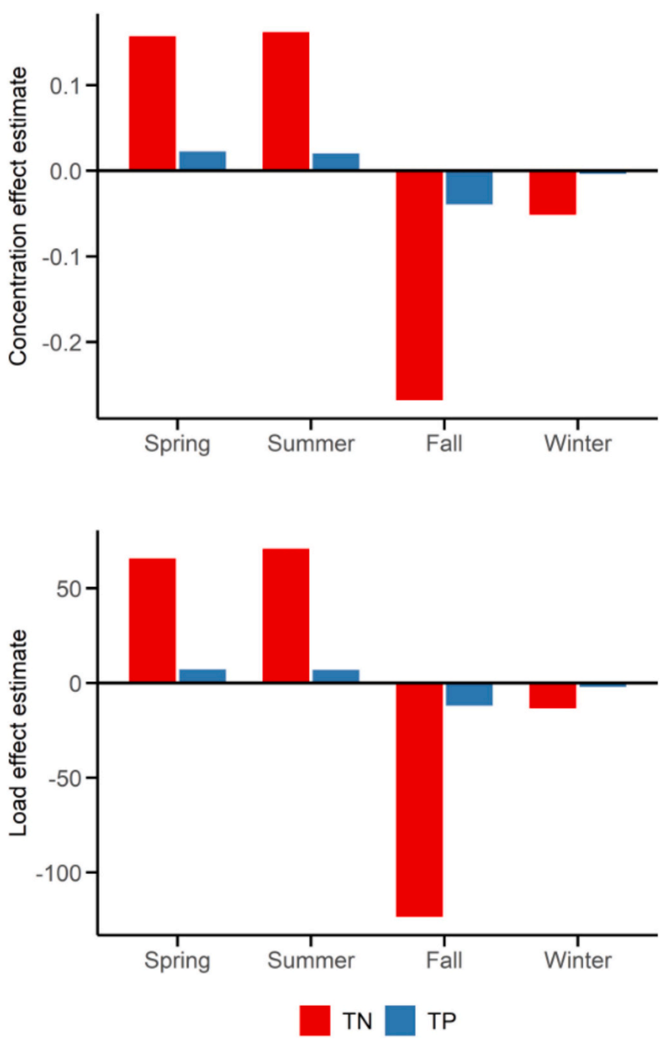

Fig. 4. GAMMs–estimated seasonal random effects for TN and TP concentrations and loads, expressed as deviations from the long–term mean after accounting for discharge and temporal trends.

loads in our study is likely driven by reduced point-source inputs, as diffuse loading in the Archipelago Sea region has declined significantly only for TP (Laamanen, 2025).

The contrasting behavior of N and P further reflects their differing biogeochemical behavior. N dynamics are largely controlled by biological processes such as nitrification and denitrification, which are sensitive to temperature, soil moisture, and redox conditions (Dai et al., 2020). On the other hand, P is governed by sorption–desorption processes, particle transport, and the mobilization of legacy P (Sharpley et al., 2013). Therefore, in catchments with long term agricultural pressure, as in our study, residual P stored in soils and sediments can buffer reductions in external inputs, delaying water quality improvements (Ekholm et al., 2015, 2007). Furthermore, the predominance of clay soils in the study catchment likely contributes to the absence of a TP trend, as clay particles strongly bind P and limit its mobilization (Puustinen et al., 2007). Similar persistence of TP has been also reported in other clay-dominated catchments in Sweden (Sandström et al., 2020). In addition, our study shows a low BFI, suggesting that most streamflow is contributed by surface hydrological process, especially during spring snowmelt when soils remain frozen (Gonzales-Inca et al., 2018). Furthermore, most agricultural fields located on clay soils are equipped with tile drainage systems, which can further enhance rapid nutrient export during runoff events. The BFI appears to be a useful proxy for inferring the relative contributions of surface runoff and groundwater to streamflow and nutrient transport, as demonstrated in several studies (Bloomfield et al., 2021; Saedi et al., 2022). However, its effectiveness may depend on catchment size and hydrological complexity (Song et al., 2022).

Hydrological control by discharge has also a dominant role in nutrient export. For example, discharge accounts for approximately 75% and 93% of TN and TP loads to the Baltic Sea, respectively (HELCOM, 2019). Our results revealed strong correlations between discharge and nutrient concentrations in the catchment (TN: $\tau = 0.59$; TP: $\tau = 0.73$, $p < 0.001$), explaining why non-normalized annual nutrient loads did not exhibit significant long-term trends.

Long-term nutrient trends can be further obscured by climate variability and seasonality, highlighting the importance of examining seasonal patterns alongside annual trends. In this study, seasonal trends in both TN and TP were more pronounced than annual trends, suggesting that climate-driven seasonal processes play a key role in shaping observed nutrient responses. The observed increase in annual and seasonal temperatures likely contributed to these patterns. Warmer conditions can extend periods of biogeochemical activity, enhancing N mineralization during summer and increasing the risk of subsequent leaching during wetter periods (Mellander et al., 2018; Øygarden et al., 2014). Elevated temperatures may also promote oxygen depletion, affecting nitrification processes and facilitating P release from sediments (Wilhelm and Adrian, 2008). Warmer winters may further reduce snow cover and soil frost, increasing particulate P transport (Räike et al., 2019), and potentially explaining the increased winter TP loads observed in this study. Together, these mechanisms provide a plausible explanation for the lack of a clear long-term TP trend despite detectable seasonal variability.

Overall, these findings indicate that nutrient responses are governed not only by long-term changes in inputs, but also by seasonal interactions among climate, hydrology, land use, and vegetation dynamics. This seasonal sensitivity helps explain why nutrient trends were more evident at sub-annual scales and provides important context for interpreting the role of land use intensity and hydroclimatic variability, which are explored in the following section.

4.2. Effect of land use intensity and hydroclimatic variability on nutrients

Our findings further highlight the distinct roles of land use intensity and hydroclimatic variability in shaping nutrient dynamics. In this study, NDVI was used as a proxy for land use intensity and seasonal vegetation activity. NDVI also reflects temporal variations in nutrient uptake, which are linked to nutrient concentrations (Zhu et al., 2015). In our study, NDVI effects were evident only in nutrient concentration models. This suggests a closer coupling between vegetation activity and nutrient availability than with nutrient transport processes.

Interannual variations in vegetation growth and vigor also influence nutrient export from land to receiving water bodies. In cold agricultural regions, growing seasons are typically short, with only one crop grown per year. As a result, year-round nutrient removal by crops is limited, and an extended non-growing season can exert a strong control on nutrient export (Liu et al., 2019a; Plach et al., 2019). Within this framework, seasonal vegetation activity plays a key role in shaping nutrient dynamics at the catchment scale by regulating nutrient uptake and mobilization.

During spring, vegetation transitions from winter dormancy to active growth. In early spring, most fields are either bare or have reduced vegetation cover, making them highly susceptible to nutrient losses through runoff. As spring progresses, vegetation growth accelerates under favorable temperature and precipitation conditions, resulting in higher greenness and increased nutrient uptake (Dai et al., 2021; Puustinen et al., 2007). This transition from nutrient mobilization to biological uptake likely explains the strong and nonlinear relationship observed between spring $NDVI_{PC1}$, representing overall vegetation activity, and TN concentration. At the same time, spring hydrological processes such as snowmelt can intensify soil erosion and sediment transport, increasing the mobilization of particulate-bound P (Liu et al., 2019b). P dynamics during spring snowmelt are therefore more strongly associated with discharge and flow pathways than with vegetation greenness, while P concentrations exhibit coherent seasonal peaks across years during the growing season regardless of flow conditions (Casson et al., 2019). These hydrologically driven processes likely explain the weak relationship observed between spring $NDVI_{PC1}$ and TP concentration.

In summer, vegetation reaches peak greenness and physiological activity stabilizes, weakening the relationship between vegetation vigor and nutrient dynamics. Under these conditions, hydroclimatic factors such as drought can become increasingly important. Drought reduces hydrological connectivity and limits erosion and nutrient transport, often resulting in lower nutrient concentrations in rivers (Giri et al., 2021; Mosley, 2015). This is consistent with the weaker, more linear relationship observed between summer $NDVI_{PC1}$ and TN concentration and with the significance of the dry spring/summer hydroclimatic class in our models. However, agricultural activity also intensifies during the summer, increasing nutrient inputs to the landscape. Therefore, nutrient losses can increase when fertilization and active crop growth coincide with precipitation events (Arvola et al., 2015; Ouyang et al., 2009).

During fall, vegetation senescence and reduced plant uptake increase N leaching potential (Pan et al., 2022). Consistent with our results, TN concentrations during this period are mainly controlled by legacy effects of accumulated biomass and residual soil N rather than active vegetation uptake. Although NDVI could not be derived for winter due to snow cover and sensor limitations, autumn NDVI provides useful information on post-harvest vegetation cover, crop residues, and soil protection. These factors strongly influence nutrient mobilization during the non-growing season. In cold regions, the non-growing season is characterized by minimal biological uptake and enhanced nutrient export driven by prolonged soil exposure, freeze–thaw cycles, and snowmelt (Liu et al., 2019a). Residual crop growth and cover crops can therefore reduce nutrient losses by limiting leaching (Liu et al., 2019c; Rutan, 2019). In our catchment, increasing winter crop cover over recent years (SVT, 2026) also suggests an improved capacity for nutrient retention during the non-growing season. In addition, delayed or reduced tillage can further limit erosion and particulate P export (Ulén et al., 2010; Uusitalo et al., 2024).

Land-use composition also modulates nutrient concentrations. Forested areas generally improve water quality by enhancing nutrient retention and biogeochemical processing, while wetland conservation or restoration effectively reduces nutrient export and increases water residence times (Rankinen et al., 2023; Syversen, 2005). In contrast, croplands are more strongly influenced by fertilization and irrigation practices, which increase nutrient availability and runoff risk (Puustinen et al., 2007). These contrasting controls are reflected in our results by the significant relationship between TN concentration and summer $NDVI_{PC2}$, which represents the contrast between forested and wetland areas and croplands.

Hydroclimatic conditions strongly regulate nutrient export by shaping hydrological connectivity and flow magnitude. Consistent with this role, our results showed that the hydroclimatic conditions were a dominant driver of nutrient loads, highlighting the critical role of hydroclimate in nutrient export. However, linking nutrient loads directly to hydroclimatic conditions can be challenging because nutrients undergo various chemical transformations and processes and are influenced by rainfall patterns, river morphology, catchment characteristics, and land cover (Kozak et al., 2019). Under both dry and wet conditions, nutrients may be either diluted or concentrated. Graham et al. (2024) found that nutrient responses during dry periods vary depending on nutrient form (dissolved vs. particulate) and dominant land use (urban vs. rural). Similarly, Arvola et al. (2015) reported that boreal rivers dominated by forestry and agriculture, such as our studied catchment, exhibited substantially lower nutrient concentrations and fluxes during low-discharge summers. Our results showed that dry conditions in spring and summer significantly reduced nutrient loads, suggesting limited transport under low-flow conditions.

Conversely, high-flow periods often lead to increased nutrient losses. Gonzales-Inca et al. (2015) documented substantial nutrient export during spring snowmelt and autumn rainfall in agricultural catchments. Similarly, Räike et al. (2019) reported that in Finnish agricultural catchments, high-flow events driven by climate variability, such as snowmelt and heavy rainfall, have maintained or even increased TN and TP export, offsetting the benefits of water protection measures. In our study of an agricultural catchment in Southwest Finland, normal fall/mild winter and wet fall/mild winter conditions were associated with significant reductions in nutrient loads, suggesting that dilution effects under high-flow scenarios can occur even in agricultural systems. This indicates that while high-flow periods often mobilize nutrients, the response may vary depending on catchment characteristics, land use, and timing of runoff events.

4.3. Limitations and future work

Reliable trend detection requires long-term, continuous data records, as trends can be obscured by high seasonal and interannual variability in nutrient loads (Gonzales-Inca et al., 2016). In this study, we utilized a 34-year time series of TN and TP, which provided valuable insights into long-term changes in water quality within the studied river catchment. Nevertheless, some uncertainty in the detected trends remains possible due to temporally sparse water quality sampling and inaccuracies in nutrient load estimation associated with the WRTDS modelling approach (Hirsch et al., 2010; Hirsch and De Cicco, 2015). Separate measurement stations for discharge and water quality introduced additional uncertainty, but likely less than other sources of uncertainty. Integrating more frequent sampling could help to identify the different drivers that regulate N and P load formation across different temporal scales and determine their relative importance.

Vegetation phenology and biomass production are dynamic processes. Although the NDVI estimated from Landsat satellite images effectively captures spatial variability, its relatively low temporal resolution limits its ability to accurately characterize the onset, duration, and senescence of vegetation growth.

We used a hydroclimatic classification based on spring/summer and fall/winter seasonal patterns to model the impact of hydroclimatic variability on nutrient loads. However, in the case of the fall/winter classification, the hydroclimatic conditions showed greater variability (Table 1), making precise categorization more difficult. To address this, we adapted and grouped certain classes, which may have introduced additional uncertainty or reduced model sensitivity. This classification adjustment is likely to have influenced the GAMMs outputs and should be considered when interpreting the results.

Our findings highlight that capturing hydroclimatic patterns over a 30-year period is complex, particularly when seasonal boundaries and climate variability shift over time. This stresses the need for future research to refine seasonal classifications or incorporate more continuous hydroclimatic variables, such as precipitation intensity, temperature anomalies, or soil moisture indices, to better represent intra-seasonal variability. Such improvements could enhance model accuracy and provide more insights into the interactions between climate, land use, and nutrient dynamics.

In addition, the model diagnostics indicated residual autocorrelation in the GAMMs for TN concentration. Several approaches were tested to address this issue, including incorporating correlation structures and alternative smoothing strategies, but none fully resolved the problem. This suggests that temporal dependence in TN concentrations may be more complex than can be captured by standard GAMM frameworks, and should therefore be considered when interpreting TN concentration responses. Future work should explore advanced time-series modelling approaches or hierarchical models that explicitly account for temporal correlation. However, TP concentration and all nutrient load models did not exhibit this issue.

5. Conclusions

This study examined how long-term changes in land use intensity and seasonal hydroclimatic variability shape nutrient dynamics in the Aurajoki catchment, Southwest Finland. Using more than three decades of monitoring data combined with remote sensing and mixed-effects modelling, the results provide new insight into the effects of land management and hydroclimate variability on N and P export.

- Flow-normalized TN loads showed a clear long-term decline, suggesting the effectiveness of improved agricultural management, reduced point source pollution, and policy interventions in reducing N export.
- TP loads remained largely stable, suggesting that P responses are buffered by soil storage, legacy effects, and particulate transport processes.
- During the study period, seasonal patterns were evident, with decreasing nutrient loads in spring and increasing loads in fall, corresponding to observed shifts in discharge regimes and seasonal temperature trends.
- NDVI effects were evident only in concentration models, reflecting the influence of vegetation dynamics on nutrient availability through plant uptake. Catchment-scale greenness was predictive of both TN and TP concentrations with summer cropland-driven N sources and forest/wetland retention processes. These results highlight the importance of forest and wetland in the mitigation of nutrient runoff. Additionally, adjusting fertilization timing and amounts based on crop growth stages could help balance productivity with environmental sustainability.
- Hydroclimatic class was a dominant driver of nutrient loads, highlighting the critical role of hydroclimate in nutrient export. Particularly, dry conditions in spring and summer, and wet conditions in fall with mild winter were significantly associated with low nutrient loads. This suggests limited transport of nutrients under dry conditions, and dilution under the wet conditions.

These results suggest that seasonal hydroclimatic variability and land use intensity play an important role in controlling nutrient dynamics, and should therefore be integrated into nutrient management strategies. Future work should focus on improving the temporal resolution of vegetation and hydrological data, integrating continuous hydroclimatic indicators, and examining the effects of extreme events to better capture short-term nutrient dynamics and land cover – climate interactions.

CRediT authorship contribution statement

Beata Plutova: Writing – review & editing, Writing – original draft, Visualization, Methodology, Investigation, Formal analysis, Data curation, Conceptualization. **Carlos Gonzales-Inca:** Writing – review & editing, Methodology, Formal analysis, Conceptualization. **Elham Kakaei Lafdani:** Writing – review & editing, Methodology, Conceptualization. **Iiro Seppä:** Writing – review & editing, Data curation. **Elina Kasvi:** Writing – review & editing, Supervision. **Maria Kämäri:** Writing – review & editing, Methodology. **Petteri Alho:** Writing – review & editing, Supervision, Funding acquisition. **Ville Kankare:** Writing – review & editing, Supervision, Conceptualization.

Declaration of generative AI and AI-assisted technologies in the writing process

During the preparation of this work the authors used ChatGPT in order to improve the linguistic clarity and readability of the manuscript, and the generation of code for statistical analysis and data visualization. After using this tool/service, the authors reviewed and edited the content as needed and take full responsibility for the content of the publication.

Declaration of competing interest

The authors declare that they have no known competing financial interests or personal relationships that could have appeared to influence the work reported in this paper.

Acknowledgments

This work was supported by the Ministry of Education and Culture's Doctoral Education Pilot, Digital Waters (DIWA) Doctoral Education Pilot (VN/3137/2024-OKM-6). Additional support was provided by the Research Council of Finland, Digital Waters Flagship Programme (359247 and 359250), and the AnthroCliMocs project (355018).

Appendix A. Supplementary data

Supplementary data to this article can be found online at https://doi.org/10.1016/j.jhydrol.2026.136012. Two supplementary tables containing additional results and supporting information related to the analyses presented in this study.

Data availability

Data will be made available on request.

All datasets analyzed in this study are publicly accessible from the sources described in Section 2 (Materials and Methods). No proprietary or restricted data were used.

References

Arvola, L., Einola, E., Järvinen, M., 2015. Landscape properties and precipitation as determinants for high summer nitrogen load from boreal catchments. Landsc. Ecol. 30, 429–442. https://doi.org/10.1007/s10980-015-0166-8.

Bamal, A., Uddin, M.G., Olbert, A.I., 2025. Assessing the impact of hydro-climatic factors on surface water quality: a global review and synthesis. J. Hydrol.: Reg. Stud. 61, 102677. https://doi.org/10.1016/j.ejrh.2025.102677.

Bloomfield, J.P., Gong, M., Marchant, B.P., Coxon, G., Addor, N., 2021. How is baseflow index (bfi) impacted by water resource management practices? Hydrol. Earth Syst. Sci. 25, 5355–5379. https://doi.org/10.5194/hess-25-5355-2021.

Boustead, B.E.M., Hilberg, S.D., Shulski, M.D., Hubbard, K.G., 2015. The accumulated winter season severity index (AWSSI). J. Appl. Meteorol. Climatol. 54, 1693–1712. https://doi.org/10.1175/JAMC-D-14-0217.1.

Casson, N.J., Wilson, H.F., Higgins, S.M., 2019. Hydrological and seasonal controls of phosphorus in northern great plains agricultural streams. J. Environ. Qual. 48, 978–987. https://doi.org/10.2134/jeq2018.07.0281.

Dai, Q., Cui, C.F., Yao, Y.F., Wang, S., Peng, M.L., Li, W.X., Zhang, Q.Q., 2021. Spatio-temporal variation of NDVI and its response to climate change in the loess plateau from 2000 to 2017. Taiwan Water Conservancy 69, 57–72. https://doi.org/10.6937/TWC.202112/PP_69(4).0004.

Dai, Z., Yu, M., Chen, H., Zhao, H., Huang, Y., Su, W., Xia, F., Chang, S.X., Brookes, P.C., Dahlgren, R.A., Xu, J., 2020. Elevated temperature shifts soil N cycling from microbial immobilization to enhanced mineralization, nitrification and denitrification across global terrestrial ecosystems. Glob. Chang. Biol. 26, 5267–5276. https://doi.org/10.1111/gcb.15211.

Dodds, W.K., Smith, V.H., 2016. Nitrogen, phosphorus, and eutrophication in streams. Inland Waters 6, 155–164. https://doi.org/10.5268/IW-6.2.909.

Ekholm, P., Granlund, K., Kauppila, P., Mitikka, S., Niemi, J., Rankinen, K., Räike, A., Räsänen, J., 2007. Influence of EU policy on agricultural nutrient losses and the state of receiving surface waters in Finland.

Ekholm, P., Rankinen, K., Rita, H., Räike, A., Sjöblom, H., Raateland, A., Vesikko, L., Cano Bernal, J.E., Taskinen, A., 2015. Phosphorus and nitrogen fluxes carried by 21 finnish agricultural rivers in 1985–2006. Environ. Monit. Assess. 187. https://doi.org/10.1007/s10661-015-4417-6.

Giri, S., Mishra, A., Zhang, Z., Lathrop, R.G., Alnahit, A.O., 2021. Meteorological and hydrological drought analysis and its impact on water quality and stream integrity. Sustainability (Switzerland) 13. https://doi.org/10.3390/su13158175.

Giri, S., Qiu, Z., 2016. Understanding the relationship of land uses and water quality in twenty first century: a review. J. Environ. Manage. 173, 41–48. https://doi.org/10.1016/j.jenvman.2016.02.029.

Gonzales-Inca, C., Valkama, P., Lill, J.O., Slotte, J., Hietaharju, E., Uusitalo, R., 2018. Spatial modelling of sediment transfer and identification of sediment sources during snowmelt in an agricultural watershed in boreal climate. Sci. Total Environ. 612, 303–312. https://doi.org/10.1016/j.scitotenv.2017.08.142.

Gonzales-Inca, C.A., Kalliola, R., Kirkkala, T., Lepistö, A., 2015. Multiscale landscape pattern affecting on stream water quality in agricultural watershed, SW Finland. Water Resour. Manag. 29, 1669–1682. https://doi.org/10.1007/s11269-014-0903-9.

Gonzales-Inca, C.A., Lepistö, A., Huttula, T., 2016. Trend detection in water-quality and load time-series from agricultural catchments of Yläneenjoki and Pyhäjoki, SW Finland.

Gorelick, N., Hancher, M., Dixon, M., Ilyushchenko, S., Thau, D., Moore, R., 2017. Google earth engine: planetary-scale geospatial analysis for everyone. Remote Sens. Environ. 202, 18–27. https://doi.org/10.1016/j.rse.2017.06.031.

Graham, D.J., Bierkens, M.F.P., van Vliet, M.T.H., 2024. Impacts of droughts and heatwaves on river water quality worldwide. J. Hydrol. (Amst) 629. https://doi.org/10.1016/j.jhydrol.2023.130590.

HELCOM, 2023. State of the Baltic Sea. Third HELCOM holistic assessment 2016-2021. Baltic Sea Environment Proceedings n°194.

HELCOM, 2021. Baltic Sea Action Plan. Updated 2021.

HELCOM, 2019. Inputs of nutrients to the sub-basins of the Baltic Sea. HELCOM core indicator report.

Hirsch, R.M., De Cicco, L.A., 2015. User guide to exploration and graphics for RivEr Trends (EGRET) and dataRetrieval: R packages for hydrologic data. Techniques and Methods. https://doi.org/10.3133/tm4A10.

Hirsch, R.M., J.R.S. and R.A.S., 1982. Techniques of trend analysis for monthly water quality data. Water Resources Research 18, 107–121.

Hirsch, R.M., Moyer, D.L., Archfield, S.A., 2010. Weighted regressions on time, discharge, and season (WRTDS), with an application to Chesapeake Bay river inputs. J. Am. Water Resour. Assoc. 46, 857–880. https://doi.org/10.1111/j.1752-1688.2010.00482.x.

Hirsch, R.M., R.B.A. and R.A.S., 1991. Selection of methods for the detection and estimation of trends in water quality. Water Resources Research 27, 803–813. https://doi.org/10.1029/91WR00259.

Hoffman, A.R., Polebitski, A.S., Penn, M.R., Busch, D.L., 2019. Long-term variation in agricultural edge-of-field phosphorus transport during snowmelt, rain, and mixed runoff events. J. Environ. Qual. 48, 931–940. https://doi.org/10.2134/jeq2018.11.0420.

Huang, S., Tang, L., Hupy, J.P., Wang, Y., Shao, G., 2021. A commentary review on the use of normalized difference vegetation index (NDVI) in the era of popular remote sensing. J. For. Res. (Harbin). https://doi.org/10.1007/s11676-020-01155-1.

Huttunen, I., Hyytiäinen, K., Huttunen, M., Sihvonen, M., Veijalainen, N., Korppoo, M., Heiskanen, A.S., 2021. Agricultural nutrient loading under alternative climate, societal and manure recycling scenarios. Sci. Total Environ. 783. https://doi.org/10.1016/j.scitotenv.2021.146871.

IPCC, 2013. Climate Change 2013: The Physical Science Basis. Contribution of Working Group I to the Fifth Assessment Report of the Intergovernmental Panel on Climate Change. Cambridge, United Kingdom and New York, NY, USA.

IPCC, 2007. Climate Change 2007: The Physical Science Basis. Cambridge.

Jolliffe, I., 2011. Principal component analysis. In: Lovric, M. (Ed.), International Encyclopedia of Statistical Science. Springer, Berlin, Heidelberg, pp. 1094–1096.

Jylhä, K., Tuomenvirta, H., Ruosteenoja, K., Niemi-Hugaerts, H., Keisu, K., Karhu, J.A., 2010. Observed and projected future shifts of climatic zones in Europe and their use to visualize climate change information. Weather Clim. Soc. 2, 148–167. https://doi.org/10.1175/2010WCAS1010.1.

Knuuttila, S., Räike, A., Ekholm, P., Kondratyev, S., 2017. Nutrient inputs into the Gulf of Finland: trends and water protection targets. J. Mar. Syst. 171, 54–64. https://doi.org/10.1016/j.jmarsys.2016.09.008.

Kozak, C., Fernandes, C.V.S., Braga, S.M., do Prado, L.L., Froehner, S., Hilgert, S., 2019. Water quality dynamic during rainfall episodes: integrated approach to assess diffuse pollution using automatic sampling. Environ. Monit. Assess. 191. https://doi.org/10.1007/s10661-019-7537-6.

Kronvang, B., Wendland, F., Kovar, K., Fraters, D., 2020. Land use and water quality. Water (Switzerland). https://doi.org/10.3390/W12092412.

Kyllmar, K., Bechmann, M., Blicher-Mathiesen, G., Fischer, F.K., Fölster, J., Iital, A., Lagzdiņš, A., Povilaitis, A., Rankinen, K., 2023. Nitrogen and phosphorus losses in Nordic and Baltic agricultural monitoring catchments – spatial and temporal variations in relation to natural conditions and mitigation programmes. Catena (Amst). 230. https://doi.org/10.1016/j.catena.2023.107205.

Laamanen, M., 2025. Assessment of HELCOM Hot Spot No. 10 Agricultural runoff to the Archipelago Sea with the view to delete the Hot Spot by 2027.

Li, L., Maier, H.R., Lambert, M.F., Simmons, C.T., Partington, D., 2013. Framework for assessing and improving the performance of recursive digital filters for baseflow estimation with application to the Lyne and Hollick filter. Environ Model Softw. 41, 163–175. https://doi.org/10.1016/j.envsoft.2012.11.009.

Liu, J., Baulch, H.M., Macrae, M.L., Wilson, H.F., Elliott, J.A., Bergström, L., Glenn, A.J., Vadas, P.A., 2019a. Agricultural water quality in cold climates: processes, drivers, management options, and research needs. J. Environ. Qual. 48, 792–802. https://doi.org/10.2134/jeq2019.05.0220.

Liu, J., Djodjic, F., Ulén, B., Aronsson, H., Bechmann, M., Bergström, L., Krogstad, T., Kyllmar, K., 2025. Toward better targeting of mitigation measures for reducing phosphorus losses from land to water: andrew Sharpley's legacy in Norway and Sweden. J. Environ. Qual. 54, 777–787. https://doi.org/10.1002/jeq2.20558.

Liu, J., Elliott, J.A., Wilson, H.F., Baulch, H.M., 2019b. Impacts of soil phosphorus drawdown on snowmelt and rainfall runoff water quality. J. Environ. Qual. 48, 803–812. https://doi.org/10.2134/jeq2018.12.0437.

Liu, J., Macrae, M.L., Elliott, J.A., Baulch, H.M., Wilson, H.F., Kleinman, P.J.A., 2019c. Impacts of cover crops and crop residues on phosphorus losses in cold climates: a review. J. Environ. Qual. 48, 850–868. https://doi.org/10.2134/jeq2019.03.0119.

LUKE, 2025a. Yields of cultivated crops by municipality [WWW Document]. Natural Resources Institute Finland (LUKE). URL https://statdb.luke.fi/PxWeb/pxweb/en/LUKE/LUKE_02%20Maatalous_04%20Tuotanto_14%20Satotilasto/01a_Viljelykasvien_sato_mk.px/ (accessed 7.30.25).

LUKE, 2025b. Number of livestock in spring by municipality [WWW Document]. Natural Resources Institute Finland (LUKE). URL https://statdb.luke.fi/PxWeb/pxweb/fi/LUKE/LUKE_02%20Maatalous_04%20Tuotanto_12%20Kotielainten%20lukumaara/01d_Kotielainten_lukumaara_kevaalla_kunta.px/ (accessed 7.30.25).

Marttila, H., Karjalainen, S.M., Kuoppala, M., Nieminen, M.L., Ronkanen, A.K., Kløve, B., Hellsten, S., 2018. Elevated nutrient concentrations in headwaters affected by drained peatland. Sci. Total Environ. 643, 1304–1313. https://doi.org/10.1016/j.scitotenv.2018.06.278.

McDowell, R.W., Luo, D., Pletnyakov, P., Upsdell, M., Dodds, W.K., 2025. Anthropogenic nutrient inputs cause excessive algal growth for nearly half the world's population. Nat. Commun. 16. https://doi.org/10.1038/s41467-025-57054-8.

Mckee, T.B., Doesken, N.J., Kleist, J., 1993. The relationship of drought frequency and duration to time scales. Eighth Conference on Applied Climatology.

McLeod, A.I., 2011. Kendall: Kendall rank correlation and Mann–Kendall trend test [WWW Document]. R package version 2.2. URL https://CRAN.R-project.org/package=Kendall (accessed 4.9.25).

Mellander, P.E., Jordan, P., Bechmann, M., Fovet, O., Shore, M.M., McDonald, N.T., Gascuel-Odoux, C., 2018. Integrated climate-chemical indicators of diffuse pollution from land to water. Sci. Rep. 8. https://doi.org/10.1038/s41598-018-19143-1.

Mosley, L.M., 2015. Drought impacts on the water quality of freshwater systems; review and integration. Earth Sci. Rev. https://doi.org/10.1016/j.earscirev.2014.11.010.

Nagy, E.D., Szilagyi, J., Torma, P., 2024. Calibrating the lyne-hollick filter for baseflow separation based on catchment response time. J. Hydrol. (Amst) 638. https://doi.org/10.1016/j.jhydrol.2024.131483.

Ngatia, L., M. Grace III, J., Moriasi, D., Taylor, R., 2019. Nitrogen and Phosphorus Eutrophication in Marine Ecosystems, in: Monitoring of Marine Pollution. IntechOpen. https://doi.org/10.5772/intechopen.81869.

Nieminen, M., Palviainen, M., Sarkkola, S., Laurén, A., Marttila, H., Finér, L., 2018. A synthesis of the impacts of ditch network maintenance on the quantity and quality of runoff from drained boreal peatland forests. Ambio. https://doi.org/10.1007/s13280-017-0966-y.

NLS, 2016. Elevation model 2019, 10 m x 10 m (Version 1) [WWW Document]. CSC – IT Center for Science. National Land Survey of Finland (NLS). URL http://urn.fi/urn:nbn:fi:csc-kata00001000000000000622 (accessed 4.9.25).

Norrgård, S., Helama, S., 2022. Tricentennial trends in spring ice break-ups on three rivers in northern Europe. Cryosphere 16, 2881–2898. https://doi.org/10.5194/tc-16-2881-2022.

Ouyang, W., Wang, X., Hao, F., Srinivasan, R., 2009. Temporal-spatial dynamics of vegetation variation on non-point source nutrient pollution. Ecol. Model. 220, 2702–2713. https://doi.org/10.1016/j.ecolmodel.2009.06.039.

Øygarden, L., Deelstra, J., Lagzdins, A., Bechmann, M., Greipsland, I., Kyllmar, K., Povilaitis, A., Iital, A., 2014. Climate change and the potential effects on runoff and nitrogen losses in the Nordic-Baltic region. Agric. Ecosyst. Environ. 198, 114–126. https://doi.org/10.1016/j.agee.2014.06.025.

Pan, F.F., Tang, J., Chen, B.H., 2022. Cover crop effects on Soil N retention and supply in fertilizer-intensive cropping systems (a review). Eurasian Soil Sci. 55, 1278–1294. https://doi.org/10.1134/S1064229322090125.

Plach, J., Pluer, W., Macrae, M., Kompanizare, M., McKague, K., Carlow, R., Brunke, R., 2019. Agricultural edge-of-field phosphorus losses in Ontario, Canada: importance of the nongrowing season in cold regions. J. Environ. Qual. 48, 813–821. https://doi.org/10.2134/jeq2018.11.0418.

Pohlert, T., 2020. trend: Non-Parametric Trend Tests and Change-Point Detection [WWW Document]. R package version 1.1.4. URL https://CRAN.R-project.org/package=trend (accessed 4.9.25).

Puustinen, M., Tattari, S., Koskiaho, J., Linjama, J., 2007. Influence of seasonal and annual hydrological variations on erosion and phosphorus transport from arable areas in Finland. Soil Tillage Res. 93, 44–55. https://doi.org/10.1016/j.still.2006.03.011.

R Core Team, 2025. R: A Language and Environment for Statistical Computing [WWW Document]. R Foundation for Statistical Computing, Vienna, Austria. URL https://www.R-project.org/ (accessed 2.3.25).

Räike, A., Taskinen, A., Knuuttila, S., 2019. Nutrient export from finnish rivers into the Baltic Sea has not decreased despite water protection measures. Ambio 49, 460–474. https://doi.org/10.1007/s13280-019-01217-7.

Rankinen, K., Cano Bernal, J.E., Holmberg, M., Vuorio, K., Granlund, K., 2019. Identifying multiple stressors that influence eutrophication in a finnish agricultural river. Sci. Total Environ. 658, 1278–1292. https://doi.org/10.1016/j.scitotenv.2018.12.294.

Rankinen, K., Futter, M., Bhattacharjee, J., Cano Bernal, J.E., Lannergård, E.E., Ojanen, M., Ronkanen, A.-K., Marttila, H., Hellsten, S., 2023. Influence of forest management changes and reuse of peat production areas on water quality in a northern river. Catena (Amst). 226, 107045. https://doi.org/10.1016/j.catena.2023.107045.

Rankinen, K., Keinänen, H., Cano Bernal, J.E., 2016. Influence of climate and land use changes on nutrient fluxes from Finnish rivers to the Baltic Sea. Agric. Ecosyst. Environ. 216, 100–115. https://doi.org/10.1016/j.agee.2015.09.010.

Röman, E., Ekholm, P., Tattari, S., Koskiaho, J., Kotamäki, N., 2018. Catchment characteristics predicting nitrogen and phosphorus losses in Finland. River Res. Appl. 34, 397–405. https://doi.org/10.1002/rra.3264.

Ruosteenoja, K., Jylhä, K., 2021. Projected climate change in Finland during the 21 st century calculated from CMIP6 model simulations.

Rutan, J., S.K., 2019. Integrating corn nitrogen management strategies and cover crops following winter wheat. Crops & Soils 52, 18–21. https://doi.org/10.2134/cs2019.52.0606.

Saedi, J., Sharifi, M.R., Saremi, A., Babazadeh, H., 2022. Assessing the impact of climate change and human activity on streamflow in a semiarid basin using precipitation and baseflow analysis. Sci. Rep. 12. https://doi.org/10.1038/s41598-022-13143-y.

Sandström, S., Futter, M.N., Kyllmar, K., Bishop, K., O'Connell, D.W., Djodjic, F., 2020. Particulate phosphorus and suspended solids losses from small agricultural catchments: links to stream and catchment characteristics. Sci. Total Environ. 711. https://doi.org/10.1016/j.scitotenv.2019.134616.

Schürings, C., Globevnik, L., Lemm, J.U., Psomas, A., Snoj, L., Hering, D., Birk, S., 2024. River ecological status is shaped by agricultural land use intensity across Europe. Water Res. 251. https://doi.org/10.1016/j.watres.2024.121136.

Seppä, I., Gonzales Inca, C., Uusikivi, J., Alho, P., n.d. CAMELS-FI: hydrometeorological time series and landscape properties for 320 catchments in Finland. Earth Syst. Sci. Data Discuss. [preprint]. https://doi.org/10.5281/zenodo.15853357.

Sharpley, A., Jarvie, H.P., Buda, A., May, L., Spears, B., Kleinman, P., 2013. Phosphorus legacy: overcoming the effects of past management practices to mitigate future water quality impairment. J. Environ. Qual. 42, 1308–1326. https://doi.org/10.2134/jeq2013.03.0098.

Song, J.H., Her, Y., Guo, T., 2022. Quantifying the contribution of direct runoff and baseflow to nitrogen loading in the Western Lake Erie Basins. Sci. Rep. 12. https://doi.org/10.1038/s41598-022-12740-1.

Stålnacke, P., Aakerøy, P.A., Blicher-Mathiesen, G., Iital, A., Jansons, V., Koskiaho, J., Kyllmar, K., Lagzdins, A., Pengerud, A., Povilaitis, A., 2014. Temporal trends in nitrogen concentrations and losses from agricultural catchments in the Nordic and Baltic countries. Agric. Ecosyst. Environ. 198, 94–103. https://doi.org/10.1016/j.agee.2014.03.028.

Sun, H., Tian, Y., Li, L., Zhuang, Y., Zhou, X., Zhang, H., Zhan, W., Zuo, W., Luan, C., Huang, K., 2024. Unraveling spatial patterns and source attribution of nutrient transport: towards optimal best management practices in complex river basin. Sci. Total Environ. 906. https://doi.org/10.1016/j.scitotenv.2023.167686.

SVT, 2026. Suomen virallinen tilasto (SVT): Viljelysmaan hoito ja kastelu [WWW Document]. Helsinki, Luonnonvarakeskus. URL https://www.luke.fi/fi/tilastot/viljelysmaan-hoito-ja-kastelu (accessed 4.30.26).

Syke, 2025a. Open environmental information systems. Hertta information system [WWW Document]. Finnish Environmental Institute (Syke). URL https://www.syke.fi/en/environmental-data/maps-and-information-services/open-environmental-information-systems#status-surface-waters (accessed 12.8.24).

Syke, 2025b. Downloadable spatial datasets: CORINE Land Cover [WWW Document]. Finnish Environmental Institute (Syke). URL https://www.syke.fi/en/environmental-data/downloadable-spatial-datasets#corine-land-cover (accessed 4.9.25).

Syversen, N., 2005. Effect and design of buffer zones in the Nordic climate: The influence of width, amount of surface runoff, seasonal variation and vegetation type on retention efficiency for nutrient and particle runoff, in: Ecological Engineering. Elsevier, pp. 483–490. https://doi.org/10.1016/j.ecoleng.2005.01.016.

Tattari, S., Koskiaho, J., Kosunen, M., Lepistö, A., Linjama, J., Puustinen, M., 2017. Nutrient loads from agricultural and forested areas in Finland from 1981 up to 2010—can the efficiency of undertaken water protection measures seen? Environ. Monit. Assess. 189. https://doi.org/10.1007/s10661-017-5791-z.

Ulén, B., Aronsson, H., Bechmann, M., Krogstad, T., Øygarden, L., Stenberg, M., 2010. Soil tillage methods to control phosphorus loss and potential side-effects: a scandinavian review. Soil Use Manag. https://doi.org/10.1111/j.1475-2743.2010.00266.x.

Uusheimo, S., Tulonen, T., Huotari, J., Arvola, L., 2020. Long-term (2001–2020) nutrient transport from a small boreal agricultural watershed: hydrological control and potential of retention ponds. Water (Switzerland) 12. https://doi.org/10.3390/w12102731.

Uusitalo, R., Lemola, R., Šuštar, M., Kurkilahti, M., Kaseva, J., Turtola, E., 2024. Strategic tillage of no-till decreased surface and subsurface losses of dissolved phosphorus. J. Environ. Qual. 53, 657–668. https://doi.org/10.1002/jeq2.20612.

Varanka, S., Hjort, J., 2017. Spatio-temporal aspects of the environmental factors affecting water quality in boreal rivers. Environ. Earth Sci. 76. https://doi.org/10.1007/s12665-016-6338-2.

Varanka, S., Hjort, J., Luoto, M., 2015. Geomorphological factors predict water quality in boreal rivers. Earth Surf. Proc. Land. 40, 1989–1999. https://doi.org/10.1002/esp.3601.

Veijalainen, N., Dubrovin, T., Marttunen, M., Vehviläinen, B., 2010. Climate change impacts on water resources and lake regulation in the vuoksi watershed in finland. Water Resour. Manag. 24, 3437–3459. https://doi.org/10.1007/s11269-010-9614-z.

WFD, 2000. Water Framework Directive. Directive 2000/60/EC of the European Parliament and the Council of 23 October 2000 establishing a framework for community action in the field of water policy.

Wilhelm, S., Adrian, R., 2008. Impact of summer warming on the thermal characteristics of a polymictic lake and consequences for oxygen, nutrients and phytoplankton. Freshw. Biol. 53, 226–237. https://doi.org/10.1111/j.1365-2427.2007.01887.x.

Wood, S., 2000. mgcv: Mixed GAM Computation Vehicle with Automatic Smoothness Estimation [WWW Document]. R package version 1.9-4. URL https://cran.r-project.org/web/packages/mgcv (accessed 12.3.25).

Wurtsbaugh, W.A., Paerl, H.W., Dodds, W.K., 2019. Nutrients, eutrophication and harmful algal blooms along the freshwater to marine continuum. Wiley Interdiscip. Rev. Water 6. https://doi.org/10.1002/WAT2.1373.

Zhu, J., Wang, X., Zhang, L., Cheng, H., Yang, Z., 2015. System dynamics modelling of the influence of the TN/TP concentrations in socioeconomic water on NDVI in shallow lakes. Ecol. Eng. 76, 27–35. https://doi.org/10.1016/j.ecoleng.2014.06.030.